

Ultra-high oxidation potential of Ti/Cu-SnO₂ anodes fabricated by spray pyrolysis for wastewater treatment

Aqing Chen^{1*}, Xudong Zhu¹, Junhua Xi¹, Haiying Qin¹, Zhenguo Ji¹

¹ *College of Materials & Environmental Engineering, Hangzhou Dianzi University, Hangzhou 310018, P R China.*

Abstract

High oxidation potential indicates anodes have high oxidation power and high current efficiency for organics oxidation. In this paper, we prepared Ti/Cu-SnO₂ anodes using spray pyrolysis method. The Ti/Cu-SnO₂ anodes have an ultra-high oxidation potential of about 2.7 V vs NHE, suitable for use in wastewater treatment. The Ti/Cu-SnO₂ anodes exhibit the preferred orientation along (110) plane at high Cu doped concentration. First-principles calculations suggest that work function of Cu-SnO₂ increases with the Cu doping concentration. It is obtained that the preferred (110) plane and the high work function are responsible for the enhanced oxidation potential of Ti/Cu-SnO₂ anodes.

Keywords: Ti/Cu-SnO₂ anodes, Oxidation potential, Spray pyrolysis

1. Introduction

Electrochemical advanced oxidation (EAO) processes which are recognized as the next generation technologies for the wastewater treatment [1] due to the high oxidation efficiency, fast reaction rate and easy operation. The oxidation power of the anodes has great impacts on the effective of the EAO processes. For the low oxidation power anode such as IrO₂-based electrodes[2,3], the interaction between electrode and hydroxyl radical is strong, which results in a low current efficiency for organics oxidation. Compared to the low oxidation power anodes, the high oxidation power

*Corresponding author.

E-mail address: aqchen@hdu.edu.cn

anodes including SnO₂-based electrodes [4–8] and boron-doped diamond (BDD) [9,10] have weaker interaction with the hydroxyl radical leading to high current efficiency for organics oxidation. The oxidation power of the anodes is determined by oxidation potential corresponding to the onset potential of oxygen evolution.

Titanium-based SnO₂ anodes as a kind of mixed metal oxide (MMO) electrodes have gained growing attention due to the relative high oxidation potential. Intrinsic SnO₂ is an *n*-type semiconductor with poor conductivity. Used as the anodes, the conductivity of SnO₂ can be improved significantly by doping Sb or F [11–13]. It is well known that the Ti/Sb-SnO₂ anodes have the oxidation potential from 1.9 to 2.2 V [14–17] which is higher than that of other MMO electrodes. However, at present, the oxidation potential of SnO₂-based anodes is still lower than that of BDD [18], although Zn/Sb co-doping can improve the oxidation potential of SnO₂-based anodes up to 2.4 V [19].

In this present work, we demonstrate titanium-based Cu doped SnO₂ (Ti/Cu-SnO₂) anodes exhibiting a ultra-high oxidation potential of about 2.7 V (*vs* NHE) which is comparable to that of BDD (2.7 V *vs* NHE) [10]. The spray pyrolysis method as the general technique for preparing doped SnO₂ thin films [20,21] was used to fabricate the Cu doped SnO₂ anodes. Moreover, the relationship between oxidation potential and the Cu doping concentration was discussed and detailed reasons for the ultra-high oxidation potential were explored further by x-ray diffraction (XRD) analyses and density functional theory (DFT) calculations.

2. Experimental details

The Ti/Cu-SnO₂ anodes were prepared by the deposition of the Cu doped SnO₂ layer on Ti substrates of 2 cm × 2 cm using a homemade spray pyrolysis apparatus. The Ti substrates were pretreated by sandblasting and then etched in boiling 10% oxalic acid during 30 min. The precursor solutions for Cu doped SnO₂ layer were prepared by adding SnCl₄·5H₂O and Cu(NO₃)₂ into ethanol. The amount of SnCl₄·5H₂O is 8.7 g

for all samples. The Cu concentration in precursor solution is 1.1 at.%, 4.2 at.% and 8.1 at.% corresponding to sample 1 (S1), sample 2 (S2) and sample 3 (S3), respectively. The resultant solutions were sprayed on the pretreated Ti substrates at the 550 ± 5 °C temperature at which the SnO₂-based anodes have high durability [8,15]. The height between the spray nozzle and Ti substrates (3 cm) and the flow of carrier gas (100L/h) were kept fixed. For comparison, Ti/Sb-SnO₂ electrodes have been prepared with the precursor solutions containing SnCl₄·5H₂O, Sb₂O₃ and several drops of HCl. The Sn:Sb atomic ratio is 9.0:1 in the precursor solution.

The crystal structure of the Cu doped SnO₂ thin films was characterized using X-ray diffraction (XRD) diffractometer with Cu K_α radiation, with a scanning angle (2θ) range of 20° to 50°. The scanning electron microscopy (HITACHI S4800) was employed to examine the morphology of Ti/Cu-SnO₂ anodes with different Cu doping level. The cyclic voltammetry (CV) tests using a standard three electrode cell were carried out to measure the oxidation potential of Ti/Cu-SnO₂ and Ti/Sb-SnO₂ anodes. The electrolyte was 0.5 M H₂SO₄ solution. Pt plate with the area of 1×1 cm² was used as a counter electrode and Hg/Hg₂SO₄·K₂SO₄ (0.64 V vs NHE) as a reference electrode. The working electrodes were the Ti/Cu-SnO₂ and Ti/Sb-SnO₂ anodes.

3. Results and discussion

We quantify the Cu content in the anodes by energy dispersive x-ray spectroscopy (EDS). The Cu concentrations in the anodes prepared by the precursor solution with Cu content of 1.1 at.%, 4.2 at.% and 8.1 at.% are 0.5 wt.%, 1.1 wt.% and 1.9 wt.%, respectively. We measured the carrier concentrations of the Cu doped SnO₂ by a Hall effect measurement system at room temperature, as shown in Fig. 1. The carrier density in the Cu-SnO₂ decreases with Cu doping level due to the compensation of the intrinsic donors by the Cu acceptors [22]. Besides, Hall effect measurements also reveal that the conduction of Cu doped SnO₂ thin films in the present work is still *n* type.

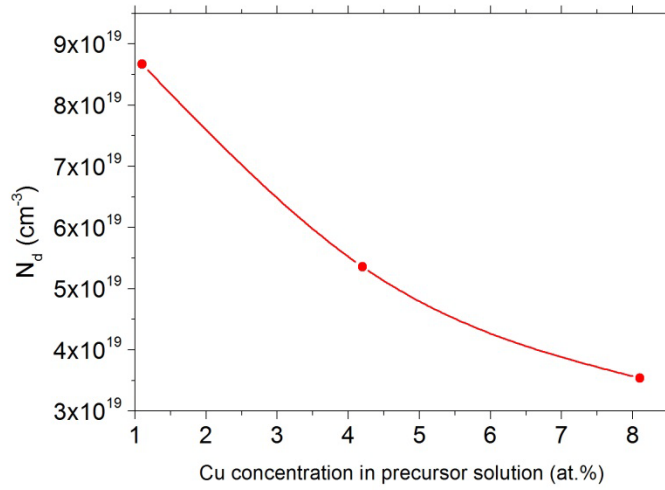


Fig. 1 the carrier density as a function of the Cu concentraion in precursor solution

Fig. 2a, 2b and 2c present the scanning electron microscopy (SEM) images of Cu-SnO₂ thin films prepared by spray pyrolysis at 550 ± 5 °C with the Cu doping concentration of 1.1 at.%, 4.2 at.% and 8.1 at.% in spray solution, respectively. No cracks on the surface of Cu-SnO₂ thin films are observed. It can be seen from Fig. 2a and 2b that the Cu-SnO₂ thin films are compact with an average particle size of ~ 0.5 μm . But the average particle size of Cu-SnO₂ thin films increases up to ~ 1 μm for the Cu doping concentration of 8.1 at.% in precursor solution. Moreover, it novel to observe that the grain become diamond-shaped, which is quiet different from the SnO₂ thin films with the Cu doping concentration of 1.1 at.% and 4.2 at.% in precursor solution. This special surface morphology can affect the oxidation potential of Ti/Cu-SnO₂ anodes, which has been proven by the the cyclic voltammograms measurements below.

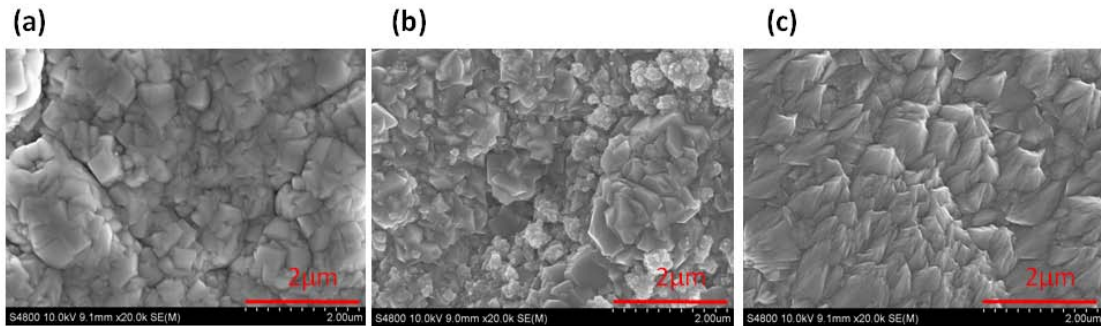


Fig. 2 SEM images of Ti/Cu-SnO₂ electrodes ($\times 20000$) with the Cu doping concentration of (a) 1.1 at.%, (b) 4.2 at.% and (c) 8.1 at.% in the precursor solution.

Fig. 3 shows the cyclic voltammograms (CV) of Ti/Sb-SnO₂ and Ti/Cu-SnO₂ electrodes in 0.5 M H₂SO₄ solution at a scan rate of 100 mV/s. It can be obtained the oxidation potential of Ti/Sb-SnO₂ is about 2.2 V vs NHE, which agrees well with reported value [23]. It is novel to find that the oxidation potential of Ti/Cu-SnO₂ is as high as 2.7 V vs NHE, which is 0.5 V bigger than that of Ti/Sb-SnO₂. It is believed that the interaction between electrode surface and hydroxyl radical determines the oxidation potential [17]. This interaction is related to the surface potential. High surface potential results in a weak interaction between electrode surface and hydroxyl radical. So, the enhanced oxidation potential suggests that the Ti/Cu-SnO₂ electrodes have high surface potential.

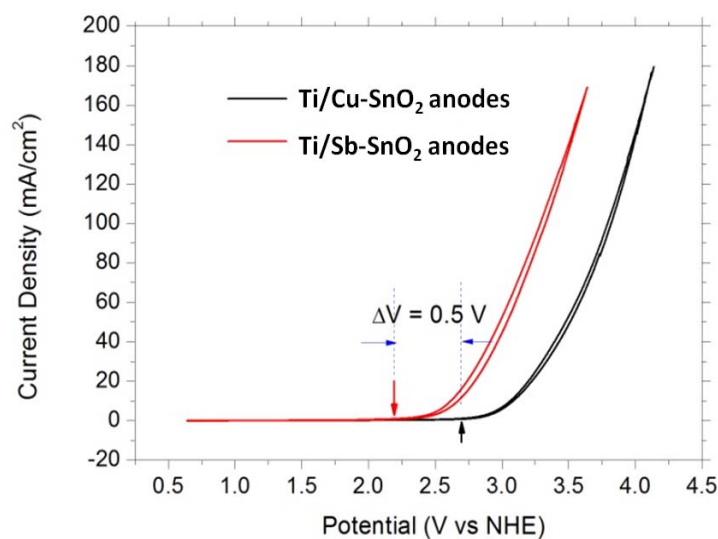


Fig. 3 Polarization curves for oxygen evolution obtained on the Ti/Cu-SnO₂ and Ti/Sb-SnO₂ electrodes in 0.5 M H₂SO₄ solution at a scan rate of 100 mV/s. For Ti/Sb-SnO₂ electrodes the Sb concentration is 10 at. % in precursor solution and for Ti/Cu-SnO₂ electrodes the Cu concentration is 8.1 at. % in precursor solution.

Fig. 4 shows the cyclic voltammograms of Ti/Cu-SnO₂ electrodes with different Cu doping concentrations. It is worth noting that the oxidation potential of S1 (V_{OP1}) is

about 2.2 V *vs* NHE which is in well agreement with that of Ti/Sb-SnO₂ electrodes. Increasing the Cu doping concentration up to 4.2 at.% leads to the oxidation potential of S2 (V_{OP2}) of about 2.6 V *vs* NHE. As the Cu doping concentration reaches 8.1 at.%, a ultra-high oxidation potential of 2.7 V *vs* NHE is obtained. So, it is obtained that the oxidation potential increases with the Cu doping concentration.

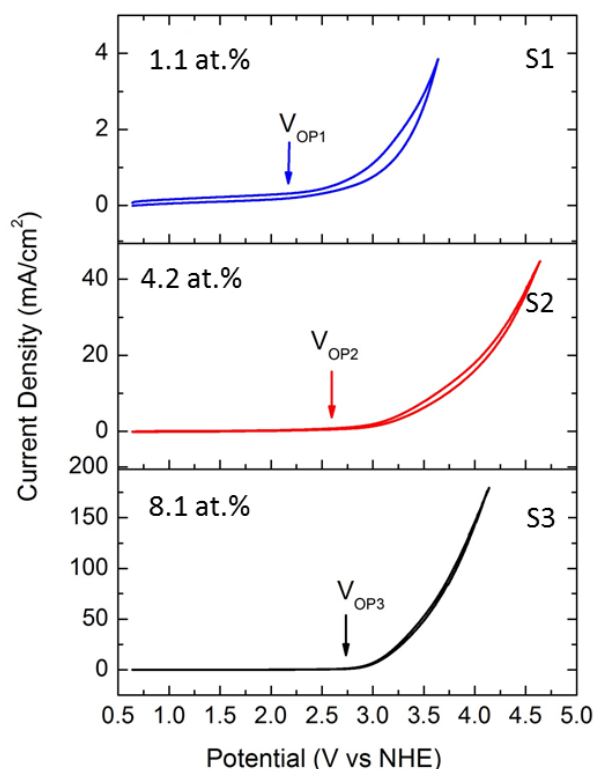


Fig. 4 Polarization curves for oxygen evolution in 0.5 M H₂SO₄ solution at a scan rate of 100 mV/s for the Ti/Cu-SnO₂ electrodes with different Cu concentrations in precursor solution (at.%). V_{OP1}, V_{OP2} and V_{OP3} are the oxidation potential of Ti/Cu-SnO₂ anodes with Cu concentrations of 1.1 at.% (S1), 4.2 at.% (S2) and 8.1 at.% (S3) in precursor solution, respectively.

As discussed above the Cu doped SnO₂ have high surface potential which is affected by surface crystal structure. In order to obtain the surface crystal structure of Cu doped SnO₂ thin films, the XRD measurements were performed on the Cu doped SnO₂ with the Cu concentration of 1.1 at. %, 4.2 at. % and 8.1 at. % in precursor solution. The XRD patterns fitted by Gaussians, as shown in Fig. 5, indicate that all of

the Cu doped SnO_2 films have the rutile structure in a good agreement with JCPD 01-070-4176 and that no impurity phase was observed. Nevertheless, Cu doping has great impacts on the crystal structure of SnO_2 . As can be seen in Fig. 5, for Ti/Cu- SnO_2 anodes with Cu concentration of 1.1 at.% and 4.2 at.% three main characteristics diffraction peaks are at 26.58° , 33.87° and 37.94° corresponding to (110), (101) and (200) planes of rutile structure of the SnO_2 phase. Moreover, it is interesting to note that the (101) peak is disappeared for Ti/Cu- SnO_2 anodes with the Cu concentrations of 8.1 at.% in precursor solution, which may result from the fact that the Cu doping changes the phase formation or cause local disorder at high concentration of 8.1 at. % in precursor solution.

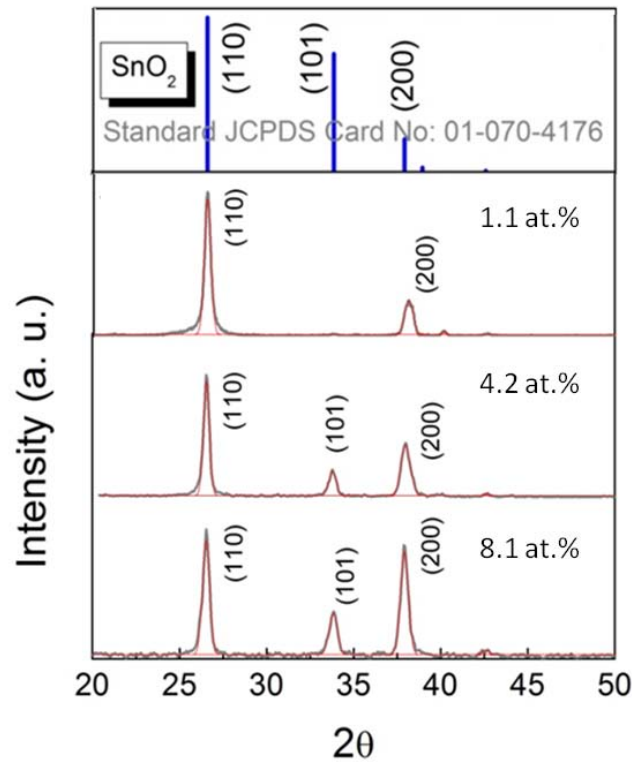


Fig .5 The XRD patterns of the Cu doped SnO_2 with the Cu concentration of 1.1 at. %, 4.2 at. % and 8.1 at. % in precursor solution in the 2θ range of 20° to 54°

In order to understand the effects of Cu doping on the crystal orientation, the texture coefficient (TC) factor [24] was calculated by the following equation:

$$TC_{(hkl)} = \frac{I_{(hkl)}/I_{0(hkl)}}{\left(\frac{1}{N}\right) \sum_{N=1}^N I_{hkl}/I_{0(hkl)}}$$

where I_{hkl} is the measured intensity value of the hkl plane and $I_{0(hkl)}$ is the standard intensity values of the hkl plane. N is the number of obtained diffraction peaks in the XRD profile. High TC_{hkl} suggests the preferred growth. Fig. 6 shows the TC_{hkl} of S1, S2, S3 and the standard SnO_2 powder (JCPD 01-070-4176). It is obvious to see that the TC_{110} increases with the Cu concentration, and on the contrary, the TC_{200} decreases with the Cu concentration. Both S1 and S2 have a preferred orientation along (200). But it novel to find that S3 exhibits a preferred orientation along (110). The surface potential is related to the crystal structure. Therefore, it is obtained that Cu doping can change the surface potential of the SnO_2 , which ultimately impacts the oxidation potential of Ti/Cu- SnO_2 electrodes.

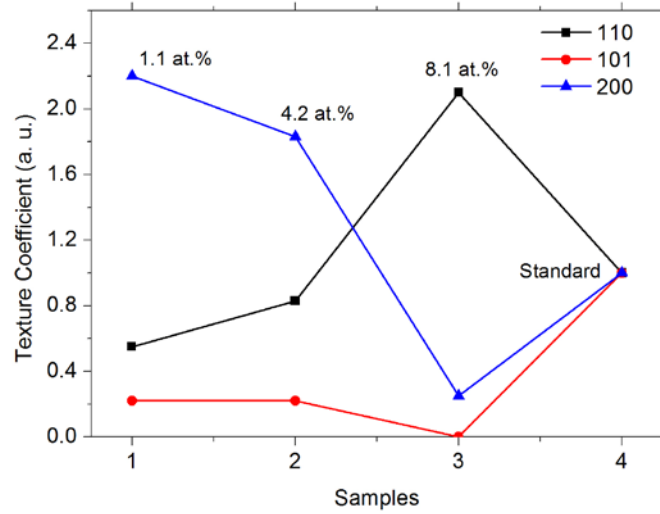


Fig .6 Variation in TC of the Cu- SnO_2 with the Cu concentration of 1.1 at. % (Sample1), 4.2 at.% (Sample2), 8.1 at.% (Sample3) in precursor solution and the standard powder (JCPD 01-070-4176, sample 4).

In order to better understand the influences of Cu doping on the oxidation potential, we performed first-principles calculations on the surface potential of SnO_2 using the Quantum ESPRESSO package [25]. The exchange-correlation energy of interacting

electrons was treated by using the Perdew-Burke-Ernzerhof generalized gradient approximation [26]. The energy cutoff for the plane-wave basis set was 40 Ry. All the models were calculated with a Monkhorst-Pack k-point (4x5x1). As shown in Fig. 7, three type structures with 7 layers separated by 20 Å vacuum layer were chosen to model the SnO₂ surface which was constructed by cleaving the SnO₂ bulk along (110) plane. They are intrinsic (Fig. 7a), one Cu atom doped (Fig. 7b) and 3 Cu atoms doped (Fig. 7c) SnO₂.

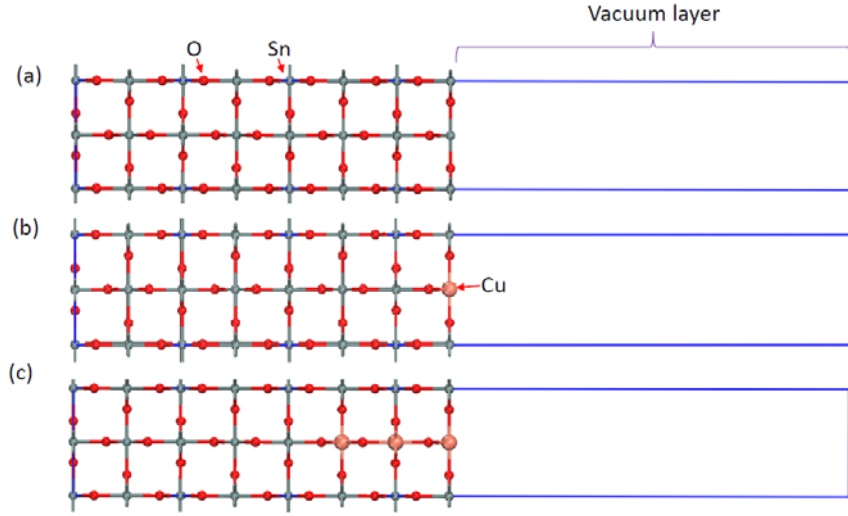


Fig. 7 the calculated models of intrinsic (a), 1 Cu atom doped (b) and 3 Cu atoms doped (c) SnO₂ were constructed by cleaving the SnO₂ bulk along (110) plane with the thickness of vacuum layer is 20 Å.

The Fermi energy level and work function Φ are the main influence factors of the surface potential. The work function which is the minimum energy needed to remove an electron from the bulk of a material through the surface to vacuum are written by

$$\phi = V_{\text{vac}} - E_{\text{F}} \quad (2)$$

where E_{F} is the Fermi level and V_{vac} is the vacuum level. Fig. 8a, 8b and 8c shows electrostatic potential energy for intrinsic, 1 Cu atom doped and 3 Cu atoms doped SnO₂, respectively. From the plot of electrostatic potential energy, we can obtain the work function of 4.46, 4.87 and 4.93 eV for intrinsic, 1 Cu atom doped and 3 Cu atoms doped SnO₂ along (110) plane, respectively. It is obvious to find that the work function increases with the Cu doping concentration. Moreover, the Fermi energy

level decreases with the Cu doping concentration, as shown in Fig. 8d. The calculated results on Fermi energy level and work functions indicate that the surface potential of SnO₂ along (110) plane increases with the Cu doping concentration.

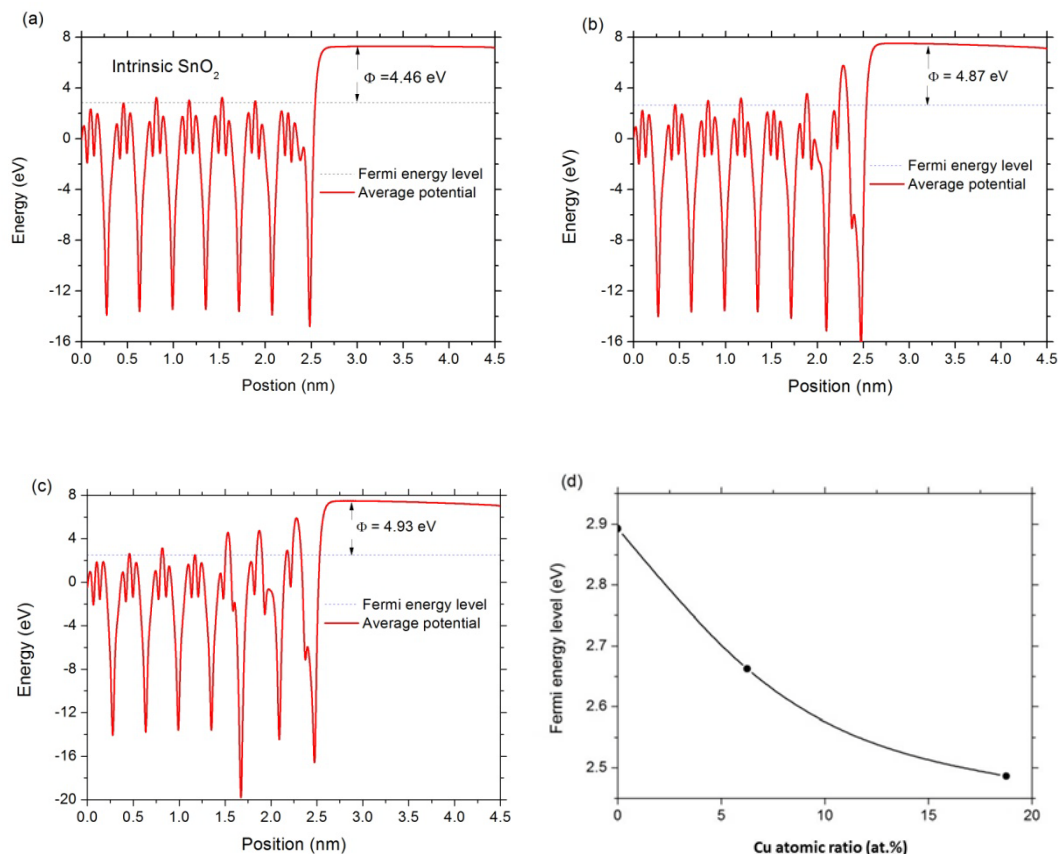


Fig.8 (a) Plane averaged electrostatic potential energy of intrinsic (a), 1 Cu atom doped (b) and 2 Cu atoms doped (c) SnO₂ surface along (110) plane, (d) Fermi energy for Cu doped SnO₂ as a function of the Cu atomic ratio.

Conclusion

In summary, we have prepared the Ti/Cu-SnO₂ anodes by spray pyrolysis method. It is found that the Ti/Cu-SnO₂ anode has an ultra-high oxidation potential of about 2.7 V vs NHE which is comparable to that of BDD. XRD data show that the Cu doped SnO₂ thin films trend to show preferred orientation along (110) as the Cu doping concentration increases. The calculated results indicate that the Fermi energy level decreases with Cu doping concentration and that the work function increases with Cu concentration, which further gives the detailed explanations on the enhancement of

oxidation potential of Ti/Cu-SnO₂ anode. These results have great significance for the development of effective SnO₂-based electrodes for wastewater treatment.

References

- [1] J. Radjenovic, D.L. Sedlak, Challenges and Opportunities for Electrochemical Processes as Next- Generation Technologies for the Treatment of Contaminated Water, *Environ. Sci. Technol.* 49 (2015) 11292–11302. doi:10.1021/acs.est.5b02414.
- [2] G. Fóti, D. Gandini, C. Comninellis, A. Perret, W. Haenni, Oxidation of Organics by Intermediates of Water Discharge on IrO₂ and Synthetic Diamond Anodes, *Electrochem. Solid-State Lett.* 2 (1999) 228–230. doi:10.1149/1.1390792.
- [3] E. Chatzisyneon, S. Fierro, I. Karafyllis, D. Mantzavinos, N. Kalogerakis, A. Katsaounis, Anodic oxidation of phenol on Ti/IrO₂ electrode: Experimental studies, *Catal. Today*. 151 (2010) 185–189. doi:http://dx.doi.org/10.1016/j.cattod.2010.02.076.
- [4] L. Xu, M. Li, W. Xu, Preparation and characterization of Ti/SnO₂-Sb electrode with copper nanorods for AR 73 removal, *Electrochim. Acta*. 166 (2015) 64–72. doi:10.1016/j.electacta.2015.02.233.
- [5] S.Y. Yang, D. Kim, H. Park, Shift of the Reactive Species in the Sb – SnO₂ – Electro catalyzed Inactivation of E. coli and Degradation of Phenol: Effects of Nickel Doping and Electrolytes, (2014). doi:10.1021/es404688z.
- [6] D. Shao, W. Yan, X. Li, H. Yang, H. Xu, A Highly Stable Ti/TiH_x/Sb–SnO₂ Anode: Preparation, Characterization and Application, *Ind. Eng. Chem. Res.* 53 (2014) 3898–3907. http://pubs.acs.org/doi/abs/10.1021/ie403768f.
- [7] T. Duan, Q. Wen, Y. Chen, Y. Zhou, Y. Duan, Enhancing electrocatalytic performance of Sb-doped SnO₂ electrode by compositing nitrogen-doped graphene nanosheets, *J. Hazard. Mater.* 280 (2014) 304–314. doi:10.1016/j.jhazmat.2014.08.018.

- [8] P. a. Christensen, K. Zakaria, H. Christensen, T. Yonar, The Effect of Ni and Sb Oxide Precursors, and of Ni Composition, Synthesis Conditions and Operating Parameters on the Activity, Selectivity and Durability of Sb-Doped SnO₂ Anodes Modified with Ni, *J. Electrochem. Soc.* 160 (2013) H405–H413. doi:10.1149/2.023308jes.
- [9] X. Chen, G. Chen, P.L. Yue, Anodic oxidation of dyes at novel Ti/B-diamond electrodes, *Chem. Eng. Sci.* 58 (2003) 995–1001. doi:10.1016/S0009-2509(02)00640-1.
- [10] X. Chen, F. Gao, G. Chen, Comparison of Ti/BDD and Ti/SnO₂-Sb₂O₅ electrodes for pollutant oxidation, *J. Appl. Electrochem.* 35 (2005) 185–191. doi:10.1007/s10800-004-6068-0.
- [11] J. Kong, S. Shi, X. Zhu, J. Ni, Effect of Sb dopant amount on the structure and electrocatalytic capability of Ti/Sb-SnO₂ electrodes in the oxidation of 4-chlorophenol, *J. Environ. Sci.* 19 (2007) 1380–1386.
- [12] D.J. Goyal, C. Agashe, B.R. Marathe, M.G. Takwale, V.G. Bhide, Effect of dopant incorporation on structural and electrical properties of sprayed SnO₂:Sb films, *J. Appl. Phys.* 73 (1993) 7520. doi:10.1063/1.354000.
- [13] G. Li, Y.-H. Wang, Q.-Y. Chen, Influence of fluoride-doped tin oxide interlayer on Ni–Sb–SnO₂/Ti electrodes, *J. Solid State Electrochem.* 17 (2013) 1303–1309. doi:10.1007/s10008-013-1997-3.
- [14] D. Shao, X. Li, H. Xu, W. Yan, An improved stable Ti/Sb–SnO₂ electrode with high performance in electrochemical oxidation processes, *RSC Adv.* 4 (2014) 21230. doi:10.1039/c4ra01990c.
- [15] B. Correa-Lozano, C. Comninellis, A. De Battisti, Service life of Ti/SnO₂–Sb₂O₅ anodes, *J. Appl. Electrochem.* 27 (1997) 970–974.
- [16] Y. Duan, Q. Wen, Y. Chen, T. Duan, Y. Zhou, Preparation and characterization of TiN-doped Ti/SnO₂-Sb electrode by dip coating for Orange II decolorization, *Appl. Surf. Sci.* 320 (2014) 746–755. doi:10.1016/j.apsusc.2014.09.182.
- [17] C. Comninellis, G. Chen, *Electrochemistry for the Environment*, 2010th ed.,

- Springer New York, New York, 2010. doi:10.1007/978-0-387-68318-8.
- [18] X. Chen, G. Chen, F. Gao, P.L. Yue, High-performance Ti/BDD electrodes for pollutant oxidation., *Environ. Sci. Technol.* 37 (2003) 5021–6.
<http://www.ncbi.nlm.nih.gov/pubmed/14620833>.
 - [19] A. Chen, B. Bin Li, B. Miljkovic, C. Souza, K. Zhu, H.E. Ruda, Improving the oxidation potential of Sb-doped SnO₂ electrode by Zn/Sb co-doping, *Appl. Phys. Lett.* 105 (2014) 021606. doi:10.1063/1.4885043.
 - [20] M. Patel, I. Mukhopadhyay, A. Ray, Molar optimization of spray pyrolyzed SnS thin films for photoelectrochemical applications, *J. Alloys Compd.* 619 (2015) 458–463. doi:10.1016/j.jallcom.2014.08.207.
 - [21] A.A. Yadav, S.C. Pawar, D.H. Patil, M.D. Ghogare, Properties of (200) oriented, highly conductive SnO₂ thin films by chemical spray pyrolysis from non-aqueous medium: Effect of antimony doping, *J. Alloys Compd.* 652 (2015) 145–152. doi:10.1016/j.jallcom.2015.08.197.
 - [22] Y. Li, R. Deng, Y. Tian, B. Yao, T. Wu, Role of donor-acceptor complexes and impurity band in stabilizing ferromagnetic order in Cu-doped SnO₂ thin films, *Appl. Phys. Lett.* 100 (2012) 172402. doi:10.1063/1.4705419.
 - [23] P. Yao, Effects of Sb doping level on the properties of Ti/SnO₂-Sb electrodes prepared using ultrasonic spray pyrolysis, *Desalination*. 267 (2011) 170–174. doi:10.1016/j.desal.2010.09.021.
 - [24] K. Ravichandran, K. Thirumurugan, N. Jabena Begum, S. Snega, Investigation of p-type SnO₂:Zn films deposited using a simplified spray pyrolysis technique, *Superlattices Microstruct.* 60 (2013) 327–335. doi:10.1016/j.spmi.2013.05.006.
 - [25] P. Giannozzi, S. Baroni, N. Bonini, M. Calandra, R. Car, C. Cavazzoni, et al., QUANTUM ESPRESSO: a modular and open-source software project for quantum simulations of materials, *J. Phys. Condens. Matter.* 21 (2009) 395502. <http://stacks.iop.org/0953-8984/21/i=39/a=395502>.
 - [26] J. Perdew, K. Burke, M. Ernzerhof, Generalized Gradient Approximation Made Simple., *Phys. Rev. Lett.* 77 (1996) 3865–3868.

<http://www.ncbi.nlm.nih.gov/pubmed/10062328>.